Chinese Chemical Letters 34 (2023) 107673

Contents lists available at ScienceDirect

Chinese Chemical Letters

journal homepage: www.elsevier.com/locate/cclet

One-step detection of T4 polynucleotide kinase activity based on single particle-confined enzyme reaction and digital particle counting

Dailu Jia[a,b], Wenjiao Fan[a,b], Wei Ren[a,b], Chenghui Liu[a,b,*]

[a] Key Laboratory of Applied Surface and Colloid Chemistry, Ministry of Education, Xi'an 710119, China
[b] Key Laboratory of Analytical Chemistry for Life Science of Shaanxi Province, School of Chemistry & Chemical Engineering, Shaanxi Normal University, Xi'an 710119, China

ARTICLE INFO

Article history:
Received 22 April 2022
Revised 22 June 2022
Accepted 8 July 2022
Available online 10 July 2022

Keywords:
T4 PNK
Single particle counting
Total internal reflection fluorescent microscope
Space-confined enzyme reaction
Nanoparticles

ABSTRACT

T4 polynucleotide kinase (T4 PNK) is a pivotal enzyme for DNA replication, recombination, and DNA damage repair. Herein, a robust single particle counting-based assay has been developed for the high-sensitive determination of T4 PNK activity through only a simple one-step reaction. Taking benefit of the exceptional space-confined enzymatic property of T4 PNK towards DNA substrates on a single nanoparticle, the T4 PNK activity can be precisely determined by counting the fluorescence-positive nanoparticles in a digital manner with a total internal reflection fluorescent microscope (TIRFM). Due to the featured spatial-confined enzymatic property of T4 PNK and the single particle counting-based signal readout, T4 PNK can be effectively differentiated from other interfering enzymes. This facile strategy has been also successfully applied to screen T4 PNK inhibitor and accurately determine T4 PNK activity in complex biological samples, paving a potential avenue for the digital analysis of biomarkers.

T4 polynucleotide kinase (T4 PNK) is a vital enzyme that can catalyze nucleic acid phosphorylation. In the existence of T4 PNK, the γ-phosphate group of adenosine triphosphate (ATP) could be transferred to the 5′-OH termini of nucleic acids [1]. An abnormal T4 PNK activity may induce the deregulation of a range of cellular activities [2], and eventually leads to serious human diseases [3–5], such as Werner syndrome, Bloom's syndrome, and Rothmund–Thomson syndrome. What is more, T4 PNK is a potential therapeutic target in cancer therapy [6]. Therefore, developing a sensitive method for the detection of T4 PNK activity is of great importance to fundamental biochemical research, drug discovery, clinical diagnosis, as well as disease treatment.

Traditional T4 PNK assays mainly depend on polyacrylamide gel electrophoresis (PAGE), radioactive isotope ^{32}P-labeling, and autoradiography [7–9]. However, these methods have several inherent shortcomings, such as radioactive hazards and complicated operations. To overcome these drawbacks, various strategies have been raised for T4 PNK analysis, such as fluorescent [10–15], colorimetric [16,17], electrochemical [18–20], chemiluminescent [21,22], and bioluminescent assays [23]. Nevertheless, most of these protocols are established with ensemble measurement-based analog signal readout modes that interrogate the averaged signal of the bulk solution, ultimately limiting the sensitivity and specificity. Notably, some elegant single entity counting-based signal readout strategies that allow for the conversion of the quantitative information of the target molecules to directly countable signals in a digital manner, have exhibited distinct advantages for biomolecule detection including enzyme analysis in terms of both high sensitivity and specificity [24–33]. Quite recently, our group has discovered that T4 PNK possesses a characteristic self-confined enzymatic property on single particles. Consequently, a microchamber-free digital strategy has been developed for quantifying T4 PNK activity by using flow cytometry [34]. Although this method effectively obtains high sensitivity for T4 PNK analysis, complex signal amplification design and multi-step operations must be involved. Therefore, exploiting simple yet sensitive digital methods is still meaningful to the accurate detection of T4 PNK activity.

Herein, taking benefit of the featured self-confined enzymatic property of T4 PNK and the single particle counting capability of the total internal reflection fluorescent microscope (TIRFM), we wish to report a robust one-step single particle counting assay for the highly sensitive quantification of T4 PNK, which is endowed with several distinct advantages. Firstly, the proposed method can be done in only one step, which greatly simplifies the assaying process, providing a fast and simple way for T4 PNK analysis. Secondly, T4 PNK can be quantified with high sensitivity by simply

* Corresponding author.
E-mail address: liuch@snnu.edu.cn (C. Liu).

https://doi.org/10.1016/j.cclet.2022.07.016
1001-8417/

counting the number of fluorescence-positive particles *via* a TIRFM imaging system. Lastly, taking benefit of the self-confined enzymatic property of T4 PNK and the particle counting-based signal transduction mode, T4 PNK can be distinguished faithfully from other interfering enzymes by investigating its featured enzymatic behaviors.

The principle of the proposed single particle counting-based T4 PNK assay is illustrated in Fig. 1. The MNP-DNA complex is composed of a streptavidin-functionalized magnetic nanoparticle (STV-MNP) anchored with DNA probe-A and probe-B. The probe-A labeled with a biotin at the 5′ ends is immobilized on the surface of the STV-MNP *via* STV-biotin conjugation. Probe-A also contains a spacer to diminish the steric hindrance, a specific sequence to hybridize with probe-B, and a TAMRA fluorophore in between of them as the reporter, respectively. Probe-B is designed to block probe-A by complementary base pairing, which has a BHQ2 at its 3′ end to efficiently quench TAMRA fluorescence on probe-A. In this way, the MNP-DNA is in a quenching state initially. According to our previous research [34], T4 PNK molecule-catalyzed phosphorylation can be spatially confined on a single particle. Therefore, when T4 PNK is introduced, it can transfer the γ-phosphate group from ATP to the 5′-OH ends of probe-B molecules step by step around a single nanoparticle. Eventually, the phosphorylated products are rapidly cleaved by λ exonuclease (λ_{exo}), which is a 5′→3′ exodeoxyribonuclease that can specifically digest probe-B from the 5′-PO_4 end of double-stranded DNA [13,35]. As such, on the T4 PNK-loaded MNPs, the quencher on probe-B will be detached from the TAMRA on probe-A, producing fluorescence-positive particles (Fig. 1a). In contrast, if T4 PNK is absent, the unphosphorylated probe-B with the 5′-OH termini will not be cleaved by λ_{exo}, which will generate fluorescence-negative particles (Fig. 1b). According to this design, the number of fluorescence-positive particles is in positive correlation to the concentration of the T4 PNK. Consequently, an accurate single particle counting assay of T4 PNK can be realized with the assistance of a TIRFM to count the number of fluorescence-positive MNPs.

For the best performance of this assay, the concentrations of λ_{exo} and ATP, and the reaction time are optimized, respectively. To investigate the effect of λ_{exo} concentration, we fix the concentration of ATP (1 mmol/L) and alter the concentration of λ_{exo} (100 U/mL to 1000 U/mL) in the samples with and without 1×10^{-3} U/mL T4 PNK. The T4 PNK-free samples are employed as the blank controls of which the signals are to be deducted when counting the number of the fluorescence-positive nanoparticles in the corresponding T4 PNK-containing samples. As shown in Fig. S1a (Supporting information), the count of fluorescence-positive particles ascends with the increasing concentration of λ_{exo} and reaches the highest value at the concentration of 500 U/mL. Then, it decreases when the λ_{exo} concentration further increases. This is because excess λ_{exo} may accelerate nonspecific DNA digestion from the 5′-OH termini on probe-B to elevate the blank control signals. Thus, 500 U/mL λ_{exo} is selected as the optimal concentration for further experiments.

The concentration of ATP is also crucial to the detection of T4 PNK because it acts as the donor of phosphate groups. To interrogate its influence, we fix the concentration of T4 PNK and λ_{exo} (1×10^{-3} U/mL and 500 U/mL, respectively) and track the number of fluorescence-positive particles with the increasing concentration of ATP. As shown in Fig. S1b (Supporting information), the count of fluorescence-positive particles gradually increases with the ascending concentration of ATP, and it reaches the highest value when the ATP concentration is 1 mmol/L. However, when the ATP concentration further ascends to 5 mmol/L and 10 mmol/L, the count of fluorescence-positive particles dramatically decreases. According to the previous report, a high concentration of ATP could inhibit DNA phosphorylation since some of the binding sites of T4 PNK may be blocked by the excess ATP [36]. As a result, 1 mmol/L is chosen as the optimal concentration for ATP.

Upon the optimized λ_{exo} and ATP concentrations, we also investigate the effect of reaction time by measuring the samples with and without T4 PNK at different time intervals. As can be seen in Fig. S1c (Supporting information), the count of fluorescence-positive particles gradually increases with the prolonged reaction time within 40 min, indicating the proceeding of the heterogeneous enzymatic reaction. Notably, if the reaction time lasts from 40 min to 50 min, the count of fluorescence-positive particles does not increase prominently. If the reaction time further extends, the background signal of the blank sample increases dramatically, which may be due to the enhanced non-specific reaction of λ_{exo}. The non-specific signals may potentially weaken the accuracy of particle counting. Hence, 40 min reaction time is employed throughout this study.

Under the optimal experimental conditions, different concentrations of T4 PNK are added to the reaction system to evaluate

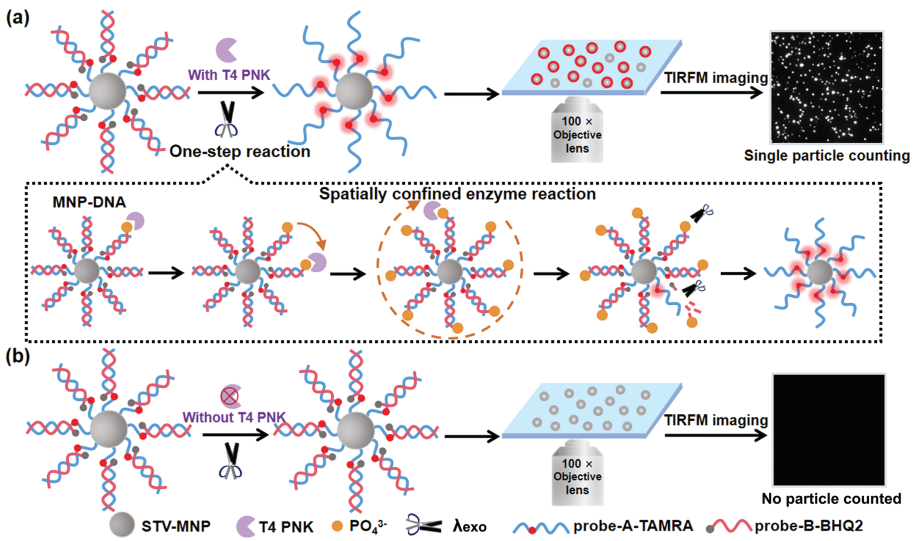

Fig. 1. The design principle of the proposed single particle counting-based T4 PNK assay. (a) Schematic workflow of the single particle counting-based assay in the presence of T4 PNK. (b) Illustration of the proposed assay in the absence of T4 PNK.

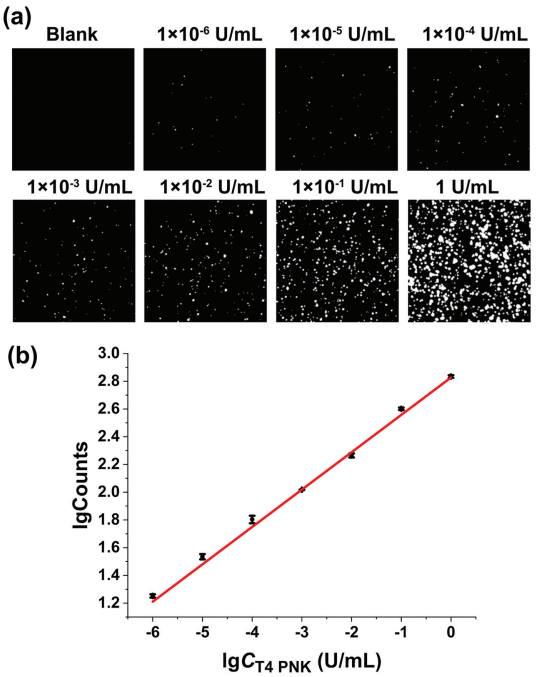

Fig. 2. Evaluating the analytical performance of the proposed T4 PNK assay. (a) TIRFM images of fluorescence-positive particles in the presence of different concentrations of T4 PNK (1×10^{-6} U/mL to 1 U/mL). (b) The relationship between the fluorescence-positive particle count and the concentration of T4 PNK. Error bars represent the standard deviation of three replicate tests.

the analytical performance of the proposed method. As Fig. 2 shows, the count of fluorescence-positive particles increases with the gradual increase of T4 PNK concentration. The logarithm of fluorescence-positive particle counts is found to vary linearly with the logarithm of T4 PNK concentration in the range from 1×10^{-6} U/mL to 1 U/mL, and as low as 1×10^{-6} U/mL T4 PNK can be clearly detected. The corresponding relationship between the T4 PNK dosage and the fluorescence-positive particle count is $\lg Counts = 0.27\ \lg C_{T4\ PNK}\ (U/mL) + 2.83$ with a correlation coefficient of $R^2 = 0.9962$. Compared with the digital flow cytometric assay reported by our group previously [34], this single particle counting method only uses a simple one-step strategy and achieves a comparable sensitivity ultimately. To the best of our knowledge, the proposed assay is one of the most sensitive methods for analyzing T4 PNK with the fewest reaction steps by far (Table S2 in Supporting information).

The specificity of our T4 PNK assay is then interrogated by detecting a collection of potential interfering enzymes, including inactive T4 PNK, T4 DNA ligase, protein kinases (PKA), hexokinase (HK), and exonuclease I (Exo I). As shown in Fig. 3, only T4 PNK produces a significant increase in fluorescence-positive particle counts, while the other interfering enzymes generate almost none. These results demonstrate that the proposed single particle counting method has excellent selectivity in the T4 PNK assay.

Exonuclease III (Exo III) is an enzyme that can recognize double-stranded DNA and gradually cleave the single nucleotides from either the blunt or the recession 3′ ends. In this way, if Exo III exists in the proposed assay system, it will randomly cleave probe-A or probe-B of the duplexes on different nanoparticles from their 3′-ends to liberate the fluorescence of TAMRA (Fig. 4a). Thus, as shown in the top panel images and histogram of Fig. 4b, the mean fluorescence intensity of all the nanoparticles treated with only Exo III will be enhanced remarkably. Therefore, as to conventional bulk measurement-based methods, if mixing Exo III with T4 PNK (1×10^{-3} U/mL) in the proposed reaction system, the interfering signals generated by Exo III can be hardly distinguished from those yielded by the target T4 PNK by setting the sample that free of both Exo III and T4 PNK as the threshold for signal collection (the bottom panel images of Fig. 4b). Fortunately, even when mixed with Exo III, T4 PNK retains its self-confined property on the nanoparticles, giving the nanoparticles more intensive fluorescence signals (Fig. 4c). Therefore, the signals produced by T4 PNK and Exo III can be distinguished by setting the signals produced by the corresponding Exo III-only samples as the thresholds respectively. In this way, when adding an equal amount of T4 PNK (1×10^{-3} U/mL) to the two reaction systems without and with 7.5×10^{-3} U/mL Exo III in parallel, by deducting the fluorescence signals yielded by the corresponding Exo III-only samples (the histogram of Fig. 4b), *i.e.*, setting the signals of Exo III-only samples as the thresholds to make the signals of each control sample just invisible (the top panel images of Fig. 4d), the counts of the fluorescence-positive nanoparticles in the two samples containing T4 PNK are almost the same (the bottom panel images and histogram of Fig. 4d). This suggests the assay will not be interfered with by Exo III by setting rational thresholds. Therefore, superior to most of the conventional methods, with the aid of the space-confined property of T4 PNK, the T4 PNK activity can be precisely determined by our proposed assay regardless of the coexistence of Exo III, which provides a promising platform for T4 PNK detection in real biological samples.

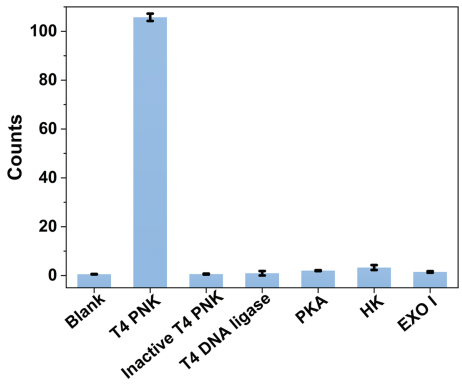

Fig. 3. Evaluating the specificity of the proposed T4 PNK assay. Fluorescence-positive particle counts produced by the blank control and the samples containing T4 PNK, heat-inactivated T4 PNK, T4 DNA ligase, PKA, HK, and Exo I, respectively. These interfering enzymes are all 1×10^{-3} U/mL in concentration. Error bars represent the standard deviation of three replicate tests.

T4 PNK is not only a critical functional enzyme but also a potential target in cancer treatment. Therefore, effective T4 PNK inhibitors may become promising drugs against cancers [6]. To evaluate the capability of this single particle counting assay in screening T4 PNK inhibitor, heparin is used as a model inhibitor [37,38]. The inhibitor screening capability of the single particle counting assay is evaluated by spiking various concentrations of heparin into the reaction system and fixing the T4 PNK concentration at 1×10^{-3} U/mL. As shown in Fig. S2 (Supporting information), the count of fluorescence-positive particles decreases with the increasing concentrations of heparin, clearly indicating the effective inhibition of T4 PNK activity. According to the experiment results, the IC_{50} value of heparin is determined to be 1.7×10^{-4} mg/mL. This value is comparable with those in literature reports by investigating the phosphatase behavior of the bi-functional T4 PNK enzyme [34,37]. This result demonstrates that this single particle counting method can be employed for T4 PNK inhibitor screening towards drug development.

Furthermore, to investigate the feasibility of the single particle counting assay in real samples, we measure the T4 PNK

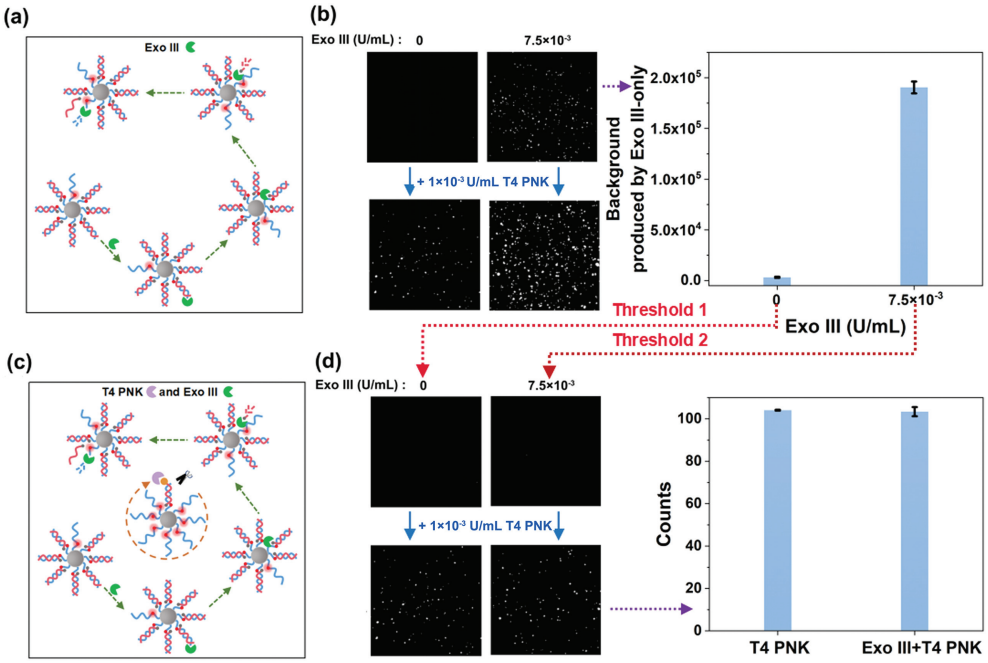

Fig. 4. (a) Principle of the Exo III cleavage process. (b) TIRFM images of the fluorescence-positive particles induced by only Exo III and the coexistence of Exo III and T4 PNK which set both T4 PNK and Exo III-free sample as the threshold (left). The fluorescent background signals produced by Exo III-only samples (right). (c) Principle for distinguishing the T4 PNK from that of Exo III. (d) TIRFM images of the fluorescence-positive particles induced by only Exo III and the coexistence of Exo III and T4 PNK which set the background signals of Exo III-only samples as the threshold (left). Counts of fluorescence-positive particles induced by T4 PNK which set the signals of Exo III-only samples as the threshold (right). Error bars represent the standard deviation of three replicate tests.

activity in nucleoproteins extracted from HeLa cells. According to the calibration curve displayed in Fig. 2, the content of T4 PNK in 60 ng nucleoproteins is determined to be 1.28×10^{-4} U/mL based on the counted number of fluorescence-positive nanoparticles. When a standard 1×10^{-4} U/mL of T4 PNK is spiked into another batch of 60 ng nucleoproteins in parallel, the final amount of T4 PNK is 2.30×10^{-4} U/mL as determined with a recovery of ~101%. Thus, this method can accurately quantify T4 PNK in complex samples, showing great potential for practical applications in clinical diagnosis and biomedical research.

In conclusion, we have developed a single particle counting assay to sensitively determine the activity of T4 PNK based on its unique space-confined kinase property. Taking advantage of the easy operating one-step strategy and the single particle resolution capability of TIRFM, simple and precise quantification of T4 PNK can be realized. What is more, based on the novel property of T4 PNK, it can be distinguished faithfully from other interfering enzymes. Considering the convenience, high sensitivity, and selectivity of this method, we believe it has great potential in T4 PNK-related clinical diagnosis and biomedical studies.

Declaration of competing interest

The authors declare that they have no known competing financial interests or personal relationships that could have appeared to influence the work reported in this paper.

Acknowledgments

This work was supported by the National Natural Science Foundation of China (Nos. 22074088, 21622507, 21904083), the Program for Changjiang Scholars and Innovative Research Team in University (No. IRT_15R43), the Innovation Capability Support Program of Shaanxi (No. 2021TD-42), and the Fundamental Research Funds for the Central Universities (Nos. GK202101001 and GK202201009) .

Supplementary materials

Supplementary material associated with this article can be found, in the online version, at doi:10.1016/j.cclet.2022.07.016.

References

[1] L.K. Wang, C.D. Lima, S. Shuman, EMBO J. 21 (2002) 3873–3880.
[2] N. Tahbaz, S. Subedi, M. Weinfeld, Nucleic Acids Res. 40 (2012) 3484–3495.
[3] J. Shen, E.C. Gilmore, C.A. Marshall, et al., Nat. Genet. 42 (2010) 245–249.
[4] J.J. Reynolds, A.K. Walker, E.C. Gilmore, C.A. Walsh, K.W. Caldecott, Nucleic Acids Res. 40 (2012) 6608–6619.
[5] S. Sharma, K.M. Doherty, R.M. Brosh, Biochem. J. 398 (2006) 319–337.
[6] S.L. Allinson, Future Oncol. 5 (2010) 1031–1042.
[7] N.K. Bernstein, R.S. Williams, M.L. Rakovszky, et al., Mol. Cell 17 (2005) 657–670.
[8] C.J. Whitehouse, R.M. Taylor, A. Thistlethwaite, et al., Cell 104 (2001) 107–117.
[9] C. Chappell, L.A. Hanakahi, F. Karimi-Busheri, M. Weinfeld, S.C. West, EMBO J. 21 (2002) 2827–2832.
[10] X. Wang, X. Chen, R.H. Zhou, et al., Anal. Chem. 93 (2021) 3889–3897.
[11] C. Feng, Z.H. Wang, T.S. Chen, et al., Anal. Chem. 90 (2018) 2810–2815.
[12] M. Liu, F. Ma, Q.Y. Zhang, C.Y. Zhang, Chem. Commun. 54 (2018) 1583–1586.
[13] Y.C. Zhang, C.H. Liu, S.J. Sun, Y.L. Tang, Z.P. Li, Chem. Commun. 51 (2015) 5832–5835.
[14] L.J. Wang, Q. Zhang, B. Tang, C.Y. Zhang, Anal. Chem. 89 (2017) 7255–7261.
[15] Y. Li, Q. Liu, L. Cui, et al., Chem. Commun. 57 (2021) 6376–6379.
[16] H.X. Jiang, D.M. Kong, H.X. Shen, Biosens. Bioelectron. 55 (2014) 133–138.
[17] C. Jiang, C. Yan, J. Jiang, R. Yu, Anal. Chim. Acta 766 (2013) 88–93.
[18] L. Cui, J. Hu, C.C. Li, C.M. Wang, C.Y. Zhang, Biosens. Bioelectron. 122 (2018) 168–174.
[19] M.H. Lin, H. Wan, J. Zhang, et al., ACS Appl. Mater. Interfaces 12 (2020) 45814–45821.
[20] L. Cui, Y. Li, M. Lu, B. Tang, C.Y. Zhang, Biosens. Bioelectron. 99 (2018) 1–7.
[21] H.Z. He, K.H. Leung, W. Wang, et al., Chem. Commun. 50 (2014) 5313–5315.
[22] W. Tang, G. Zhu, C.Y. Zhang, Chem. Commun. 50 (2014) 4733–4735.
[23] J. Du, Q. Xu, X. Lu, C.Y. Zhang, Anal. Chem. 86 (2014) 8481–8488.
[24] S. Sakamoto1, T. Komatsu1, R. Watanabe, et al., Sci. Adv. 6 (2020) eaay0888.
[25] K. Akama, K. Shirai, S. Suzuki, Anal. Chem. 88 (2016) 7123–7129.
[26] L. Cohen, M.R. Hartman, A. Amardey-Wellington, D.R. Walt, Nucleic Acids Res. 45 (2017) e137.
[27] W.J. Fan, Y. Qi, X.H. Lu, et al., Chem. Commun. 56 (2020) 7179–7182.
[28] Z. Farka, M.J. Mickert, M. Pastucha, et al., Angew. Chem. Int. Ed. 59 (2020) 10746–10773.
[29] Y.X. Lu, Z.D. Tong, Z.H. Wu, et al., Chin. Chem. Lett. 33 (2022) 3188–3192.
[30] L. Mou, H.H. Hong, X.J. Xu, Y. Xia, X.Y. Jiang, ACS Nano 15 (2021) 13077–13084.

[31] T. Tian, B.W. Shu, Y.Z. Jiang, et al., ACS Nano 15 (2021) 1167–1178.
[32] C. Wu, P.M. Garden, D.R. Walt, J. Am. Chem. Soc. 142 (2020) 12314–12323.
[33] V. Yelleswarapu, J.R. Buser, M. Haber, et al., Proc. Natl. Acad. Sci. U. S. A. 116 (2019) 4489–4495.
[34] L.J. Zhang, W.J. Fan, D.L. Jia, et al., Anal. Chem. 93 (2021) 14828–14836.
[35] K. Subramanian, W. Rutvisuttinunt, W. Scott, R.S. Myers, Nucleic Acids Res. 31 (2003) 1585–1596.
[36] Z.W. Tang, K.M. Wang, W.H. Tan, et al., Nucleic Acids Res. 33 (2005) e97.
[37] C.B. Ma, Z.W. Tang, K.M. Wang, et al., ChemBioChem 8 (2007) 1487–1490.
[38] E.A. Galburt, J. Pelletier, G. Wilson, B.L. Stoddard, Structure 10 (2002) 1249–1260.